NJC

Accepted Manuscript

This article can be cited before page numbers have been issued, to do this please use: R. ma, P. Yang and F. Bian, *New J. Chem.*, 2018, DOI: 10.1039/C7NJ05014C.


Volume 40 | Number 1 | January 2016 | Pages 1–846

NJC

New Journal of Chemistry
www.rsc.org/njc

A journal for new directions in chemistry

ISSN 1144-0546

ROYAL SOCIETY OF CHEMISTRY

PAPER
Jason B. Benedict et al
The role of atropisomers on the photo-reactivity and fatigue of diarylethene-based metal–organic frameworks

cnrs

View Article Online
DOI: 10.1039/C7NJ05014C

Journal Name

ARTICLE

Magnetic dendritic polymer nanocomposites as supports for Palladium: a highly efficient and reusable catalyst for Mizoroki-Heck and Suzuki-Miyaura coupling reactions

Received 00th January 20xx,
Accepted 00th January 20xx

DOI: 10.1039/x0xx00000x

www.rsc.org/

Rong Ma,[‡] Pengbo Yang,[‡] and Fengling Bian*

A novel catalyst Fe_3O_4@SiO_2-Dendrimer-Pd based on palladium immobilized on magnetic dendritic polymer nanocomposites was successfully synthesized and characterized by FT-IR, EA, XRD, TEM, EDX, VSM and XPS. This nanocatalyst showed excellent catalytic activity for solvent-free Mizoroki-Heck reaction and Suzuki-Miyaura reaction in EtOH/H2O at palladium loading of only 0.009 mol%. Moreover, Fe_3O_4@SiO_2-Dendrimer-Pd catalyst could be conveniently recovered by an external magnet and used consecutively for five times with excellent yields achieved. The remarkable catalytic performances and convenient magnetic separability of the Fe_3O_4@SiO_2-Dendrimer-Pd catalyst make it a promising catalyst for the practical application.

1 Introduction

Palladium-catalyzed coupling reactions are of significant importance to the straightforward and facile formation of C-C bonds in modern chemical transformations.[1] In spite of excellent catalytic activity of homogeneous Pd catalysts, it also suffers from significant drawbacks associated with tedious separation and recycling. One approach to overcome these disadvantages is heterogenization of homogeneous catalysts using a support,[2] which may cause new problems including low catalytic activity and selectivity.[3] Thus, it is highly desirable to develop more active and recylable catalysts from environmental, economical and practical points of view.

Dendritic polymers have aroused a lot of interest recently because of their unique properties such as highly branched, spherical three-dimensional macromolecules and nanometer size,[4-9] and they are particularly well-suited for hosting metal catalysts. Firstly, owing to the highly branched and three-dimensional structure, there are multiple internal and external functional groups which could coordinate with transition metals and stabilize them. Moreover, a lot of cavities, which existed in dendritic polymers because of three-dimensional structure, could absorb and concentrate reactants, and make the reaction proceed more efficiently. Finally, the nanometer size of dendrimer-stabilized metal nanoparticles can not only possess the advantages of high activity of homogeneous catalysts due to their high densities of active sites and good dispersion in common solvents, but also have the recyclability of heterogeneous catalysts by fixation on a solid support.[10] Therefore, dendritic polymers are found to be potential hosts in catalytic processes. Deraedt *et al.* prepared new catalysts by anchoring palladium nanoparticles on “click” dendrimers, and these catalyst exhibited excellent activity in C-C coupling reactions and reduction of 4-nitrophenol at parts per million level.[11]

However, the nanometer size of dendritic polymers-supported Pd catalyst has posed more difficulties for separation and recovery.[4,8] Introduction of magnetic material could be an attractive solution to this problem, which not only retains the original nano-sized, but also simplifies the procedure of separation and recycling.[12,13] Up to now, few papers have reported about magnetic dendritic polymers-supported Pd catalysts in C-C coupling reactions.[14,15] Christophe *et al.* developed a new magnetic dendritic polymer-supported Pd catalyst by simple impregnation of γ-Fe_2O_3/SiO_2 with “clicked” dendrimer-supported Pd catalyst.[7] This catalyst is magnetically separable and highly catalytic active in Suzuki-Miyaura reactions.

With the development of green chemistry and engineering, it is highly desirable to develop more heterogeneous catalysts with excellent catalytic activity and reusability in green systems. Herein we prepared a novel magnetic dendritic polymer nanocomposites-supported Pd catalyst Fe_3O_4@SiO_2-Dendrimer-Pd. This catalyst exhibits high activity for Mizoroki-Heck reaction (solvent-free) and Suzuki-Miyaura reaction (EtOH/H_2O) at low palladium loading, and could be easily separated with an external magnet and reused for five times with excellent yields achieved.

2 Experimental

2.1 Materials

College of Chemisry and Chemical Engineering, Lanzhou University, Lanzhou 730000, P.R. China. E-mail: bianfl@lzu.edu.cn

†Electronic Supplementary Information (ESI) available. See DOI: 10.1039/x0xx00000x

‡These authors contributed equally to the work.

View Article Online
DOI: 10.1039/C7NJ05014C

3,3'-Diaminodipropylamine (≥98.0%), 3-aminopropyltrimethoxysilane(APTMS, ≥96.0%) were purchased from TCI (Shanghai) Development Co., Ltd. and used as received. Iron chloride tetrahydrate ($FeCl_2·4H_2O$) and ferric chloride hexahydrate ($FeCl_3·6H_2O$) were obtained from Tianjin Guangfu Fine Chemicals. Methylacrylate (MA, ≥98.0%) was provided by Tianjin Chemical Reagent Company and purified by vacuum distillation. Ethylsilicate (TEOS) was obtained from Tianjin No.1 Chemical Reagent Factory. Palladium chloride ($PdCl_2$, ≥59.5%) was purchased from Shenyang Keda Reagents Company. Other materials were analytical grade and used without further purification.

2.2 Characterization

Fourier-transform infrared (FT-IR) spectra were recorded on a NEXUS670 (Nicolet, USA) spectrophotometer. Thermal gravimetric analysis (TGA) measurement was performed on a STA449C TGA instrument (Netzsch, Germany) with a heating rate of 10 °C min^{-1} in flowing N_2 atmosphere. Elemental analysis was measured with a Vario EL (Elementar, Germany) analyzer. Transmission electron microscopy (TEM) measurement was carried out on a Tecnai-G2-F30 (FEI, USA) under an operating voltage of 300 kV. The magnetic properties of the nanoparticles were obtained from a vibrating sample magnetometer (Lake Shore 7304, USA). X-ray diffraction (XRD) measurements were carried out at room temperature by using a Shimadzu XRD-6000 spectrometer (Japan) under nickel-filtered CuKα radiation. X-ray photoelectron spectrographs (XPS) were performed on an Axis Ultra DLD electron spectrometer (Kratos, UK) using C1s=284.4 eV signal as internal standard. The Palladium content of the supported catalyst was obtained from an AA240 (Varian Corporation, USA) atomic absorption spectrometer (AAS). ^{1}H and ^{13}C NMR (400 and 100 MHz) spectra were recorded on an AVANCE III 400 NMR spectrometer (Bruker, Germany) with $CDCl_3$ or [D$_6$]DMSO as solvents.

2.3 Preparation of Fe_3O_4@SiO_2 nanoparticles

Fe_3O_4 nanoparticles were firstly prepared by a chemical co-precipitation method in our previous work.[16a] Then 500 mg of Fe_3O_4 nanoparticles and 1 mL NH_4OH were homogenized in 50 mL of ethanol/water solvent (volume ratio of 4:1) with the help of an ultrasound mixer. Afterward, 0.5 mL of ethylsilicate (TEOS) was injected into the reaction mixture dropwise. Finally, the reaction mixture was kept at room temperature under vigorous stirring for 16 h. After the reaction was complete, the resulting nanoparticles were separated by an external magnet and washed with ethanol and water several times. the obtained product was dried under vacuum for 24 h to give the Fe_3O_4@SiO_2 nanoparticles.

2.4 Preparation of Fe_3O_4@SiO_2-NH_2 nanoparticles

Fe_3O_4@SiO_2-NH_2 were prepared according to the previous report.[17] A mixture of Fe_3O_4@SiO_2 nanoparticles (1.000 g) and 3-aminopropyltrimethoxysilane (APTMS, 2 mL) in 25 mL toluene were homogenized by an ultrasound mixer and were stirred under reflux conditions for 12 h in the argon atmosphere. Then, the reaction mixture was separated with an external magnet, and the obtained Fe_3O_4@SiO_2-NH_2 nanoparticles were washed with ethanol and acetone several times and dried under vacuum overnight.

2.5 Preparation of Fe_3O_4@SiO_2-MA1 nanoparticles

200 mg of Fe_3O_4@SiO_2-NH_2 nanoparticles were dispersed in 1 mL methanol using an ultrasound mixer. After bubbled with Ar gas for 15 min, 0.090 mL (1.0 mmol) of MA was added to the aforementioned suspension. Then, the reaction mixture was stirred at 25 °C for 24 h. Finally, the obtained product was collected by a permanent magnet, washed with methanol for three times and dried under vacuum for 12 h to give Fe_3O_4@SiO_2-MA1 nanoparticles.

2.6 Preparation of Fe_3O_4@SiO_2-MA1-NH_2(1) nanoparticles

A slurry of Fe_3O_4@SiO_2-MA1 nanoparticles (200 mg) in methanol (1 mL) was ultrasonic treated and bubbled with Ar gas for 15 min.Then, 0.280 mL (2.0 mmol) of 3,3'-diaminodipropylamine was added, and the mixture was stirred at reflux for 6 h. After washing with methanol for several times and drying, the Fe_3O_4@SiO_2-MA1-NH_2(1) nanoparticles were eventually obtained.

2.7 Preparation of Fe_3O_4@SiO_2-MA2-NH_2(2) nanoparticles

The Fe_3O_4@SiO_2-MA1-NH_2(1) nanoparticles (200 mg) were mixed with methanol (2 mL) and MA (0.180 mL, 2.0 mmol) by an ultrasound mixer. Then, the reaction mixture was stirred at room temperature for 24 h. After the reaction was complete, the Fe_3O_4@SiO_2-MA2 nanoparticles were collected with a permanent magnet, washed with methanol and then dried under vacuum. Afterward, 3,3'-diaminodipropylamine (0.560 mL, 4.0 mmol) was added to a stirred 2 mL methanol dispersion of Fe_3O_4@SiO_2-MA2 (200 mg). The final mixture was stirred at reflux for 6 h under Ar atmosphere. Final product was collected with an external magnet, washed with methanol for several times and then dried in a vacuum for 12 h to give Fe_3O_4@SiO_2-MA2-NH_2(2) nanoparticles.

2.8 Preparation of the Fe_3O_4@SiO_2-Dendrimer-Pd catalyst

The mixture of 3 mg of Fe_3O_4@SiO_2-MA2-NH_2(2) nanoparticles in 0.4 mL of $PdCl_2$ solution (0.5 mM) was stirred at room temperature for 12 h. Then, the final catalyst Fe_3O_4@SiO_2-Dendrimer-Pd was collected by a permanent magnet, washed with water for three times and dried in a vacuum.

2.9 General procedure for the solvent-free Mizoroki-Heck reactions

Aryl halides (2.0 mmol), olefin (3.0 mmol), Et_3N (3.0 mmol) and Fe_3O_4@SiO_2-Dendrimer-Pd (0.009 mol% based on aryl halides) were added into a reaction vessel. Then, the mixture was heated up to 120 °C, and stirred under Ar atmosphere for a given time. After the reaction was complete, 3 mL of ethyl acetate/ethanol (1:1, v/v) was added into the reaction vessel. The catalyst Fe_3O_4@SiO_2-Dendrimer-Pd was separated with an external magnet and washed with ethyl acetate/ethanol (1:1, v/v) (3 mL×3). Afterward, the organic phase was evaporated and purified by column chromatography with petroleum ether/ethyl acetate as eluent. The final products were analyzed by ^{1}H NMR and ^{13}C NMR spectroscopy.

View Article Online
DOI: 10.1039/C7NJ05014C

2.10 General procedure for the Suzuki-Miyaura reactions

A mixture of aryl halides (2 mmol), phenylboronic acid (2.4 mmol), K_2CO_3 (5.0 mmol) and Fe_3O_4@SiO_2-Dendrimer-Pd (0.009 mol% with respect to aryl halides) in 6 mL of EtOH/H_2O (1:1) was stirred at 75 ^{o}C under Ar atmosphere for 1 h. After the reaction was complete, the catalyst was magnetically separated and washed with ethyl acetate (3×2 mL) and water (3×2 mL). Then, the water phase was extracted with ethyl acetate (3×10 mL), and all organic phases were combined, dried over anhydrous $MgSO_4$ and evaporated. The final products were obtained by flash chromatography using petroleum ether/ethyl acetate as eluent, and analyzed by ^{1}H NMR and ^{13}C NMR spectroscopy.

2.11 General procedure for catalyst recovery

Iodobenzene (1.0 mmol), *n*-butyl acrylate (1.5 mmol), Et_3N (1.5 mmol) and Fe_3O_4@SiO_2-Dendrimer-Pd (0.018 mol% based on iodobenzene) were mixed in a reaction vessel. Then, the mixture was stirred at 120 ^{o}C for 60 min under Ar atmosphere. After the reaction was complete, the catalyst was separated with an external magnet and washed with ethyl acetate/ethanol (1:1, v/v) (3 mL×3), then dried and reused for the next run.

3 Results and discussion

The synthetic procedures of the magnetic dendritic polymer nanocomposites supported palladium catalyst Fe_3O_4@SiO_2-Dendrimer-Pd are illustrated in Scheme 1. First, Fe_3O_4 were coated with a thin layer of silica by adding NH_4OH and TEOS to afford Fe_3O_4@SiO_2 nanoparticles. Then, the Fe_3O_4@SiO_2 nanoparticles were modified with 3-aminopropyltrimethoxysilane (APTMS) by stirring at reflux for 12 h, reaping the aminopropyl-functionalized nanoparticles Fe_3O_4@SiO_2-NH_2. Next, the magnetic dendritic polymer nanocomposites Fe_3O_4@SiO_2-MA2-NH_2(2) were prepared by Fe_3O_4@SiO_2-NH_2 gradually reacting with methylacrylate and 3,3'-diaminodipropylamine for two times. Finally, the catalyst Fe_3O_4@SiO_2-Dendrimer-Pd was obtained by stirring the mixture of $PdCl_2$ solution and Fe_3O_4@SiO_2-MA2-NH_2(2) nanoparticles at room temperature. Atomic absorption spectroscopy (AAS) analysis gave a palladium loading of 0.06 mmol/g in Fe_3O_4@SiO_2-Dendrimer-Pd catalyst.

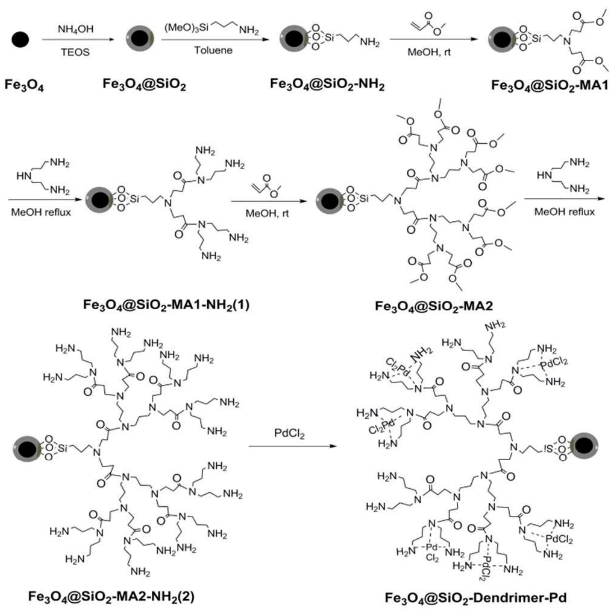

Scheme 1 Schematic of the preparation of the Fe_3O_4@SiO_2-Dendrimer-Pd catalyst.

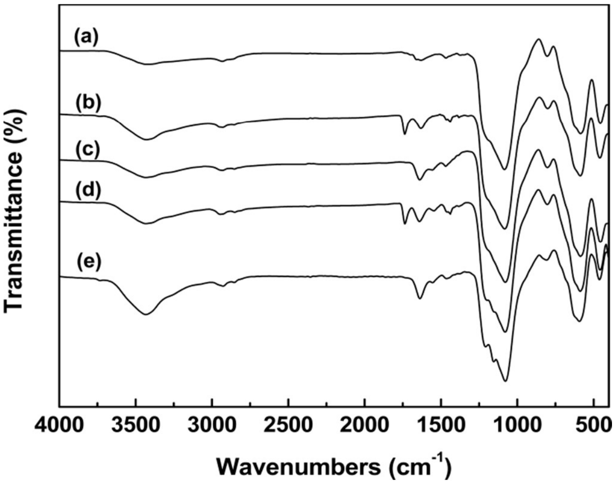

Fig. 1 FT-IR spectra of (a) Fe_3O_4@SiO_2-NH_2, (b) Fe_3O_4@SiO_2-MA1, (c) Fe_3O_4@SiO_2-MA1-NH_2(1), (d) Fe_3O_4@SiO_2-MA2, (e) Fe_3O_4@SiO_2-MA2-NH_2(2).

Fig. 1 shows the FT-IR spectra of (a) Fe_3O_4@SiO_2-NH_2, (b) Fe_3O_4@SiO_2-MA1, (c) Fe_3O_4@SiO_2-MA1-NH_2(1), (d) Fe_3O_4@SiO_2-MA2, (e) Fe_3O_4@SiO_2-MA2-NH_2(2). In Fig. 1a, the characteristic band at 586 cm^{-1} is owing to the Fe-O stretching vibration. The characteristic bands at 1084 cm^{-1}, 804 cm^{-1}, 456 cm^{-1} correspond to asymmetric, symmetric stretching vibration and bending vibration of Si-O-Si bond. The band at 1471 cm^{-1} is attributed to N-H bending vibration, and the absorption bands of aliphatic CH_2 groups could be viewed at 2932 cm^{-1}, 2869 cm^{-1}, respectively. The characteristic band of H-O-H bending vibration in water is at 1631 cm^{-1}. All of these bands confirm the successful synthesis of Fe_3O_4@SiO_2-NH_2 nanoparticles.[18,19] Compared with Fig. 1a, a new band at 1737 cm^{-1} appeared in the spectrum of Fe_3O_4@SiO_2-MA1 (Fig. 1b) and can be attributed to the C=O stretching vibration in ester groups.[20a] In Fig. 1c, the band at 1737 cm^{-1} that correspond to C=O stretching frequency of ester groups disappears while the band at 1639 cm^{-1} that attributed to the C=O stretching frequency of amide groups appears, suggesting the Fe_3O_4@SiO_2-MA1-NH_2(1) nanoparticles has been successful prepared.[6,20b] Compared with Fig. 1b and c, Fig. 1d and e showed stronger absorption bands at 1737 cm^{-1} and 1639 cm^{-1}, indicating Fe_3O_4@SiO_2-MA2 and Fe_3O_4@SiO_2-MA2-NH_2(2) were obtained.

TGA of Fe_3O_4@SiO_2-Dendrimer-Pd catalyst was performed. As shown in Fig. 2, the catalyst displays a 0.25 % weight loss at around 150 ^{o}C due to physically adsorbed moisture.[21] The main weight loss (6.04 %) was observed above 300 ^{o}C due to the degradation of organic moieties on the surface of the catalyst. Above results displayed that the Fe_3O_4@SiO_2-Dendrimer-Pd catalyst has good thermal stability and appropriate for the application in most organic reactions.

View Article Online
DOI: 10.1039/C7NJ05014C

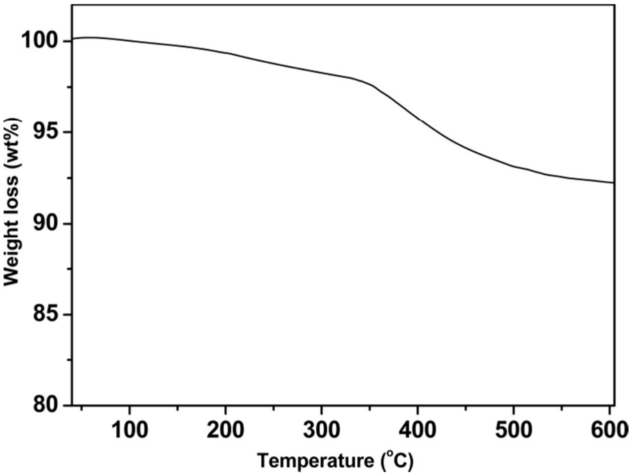

Fig. 2 TGA curves of $Fe_3O_4@SiO_2$-Dendrimer-Pd catalyst.

Table 1 Elemental analysis (EA) results

Entry	Sample	C(%)	H(%)	N(%)	Total(%)
1	$Fe_3O_4@SiO_2$-NH_2	3.270	0.760	0.720	4.750
2	$Fe_3O_4@SiO_2$-MA1-NH_2(1)	3.430	0.784	0.940	5.154
3	$Fe_3O_4@SiO_2$-MA2-NH_2(2)	4.460	0.788	1.190	6.438

^{a} Total(%) = C% + H% + N%.

The elemental analysis results of dendritic polymer nanocomposites were summarized in Table 1. The weight percentages of nitrogen and organic moieties for magnetic nanoparticles increased in the following order: $Fe_3O_4@SiO_2$-NH_2 < $Fe_3O_4@SiO_2$-MA1-NH_2(1) < $Fe_3O_4@SiO_2$-MA2-NH_2(2) (entries 1-3), suggesting the successful synthesis of magnetic nanoparticles $Fe_3O_4@SiO_2$-MA1-NH_2(1) and $Fe_3O_4@SiO_2$-MA2-NH_2 (2). The nitrogen weight of $Fe_3O_4@SiO_2$-MA2-NH_2(2) was 1.190%, indicating that there is 0.85 mmol/g of nitrogen content in the dendritic polymer nanocomposites.

The magnetic properties of obtained nanoparticles were measured by VSM at room temperature. As shown in Fig. 3, these nanoparticles of (a) $Fe_3O_4@SiO_2$, (b) $Fe_3O_4@SiO_2$-MA2-NH_2 (2) and (c) $Fe_3O_4@SiO_2$-Dendrimer-Pd exhibit superparamagnetic nature and have saturation magnetization of 54.05 emu/g, 47.47 emu/g and 45.59 emu/g respectively. Such high saturation magnetization value is enough for $Fe_3O_4@SiO_2$-Dendrimer-Pd catalyst to be separated with an external magnet, when the external magnet is removed, it could be easily dispersed in solution again. Fig. 4 shows the photograph of the magnetic separation and redispersion of $Fe_3O_4@SiO_2$-Dendrimer-Pd catalyst.

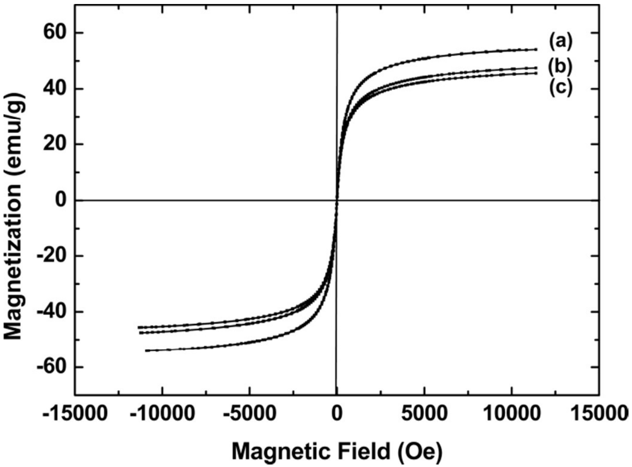

Fig. 3 Room-temperature magnetization curves of (a) $Fe_3O_4@SiO_2$, (b) $Fe_3O_4@SiO_2$-MA2-NH_2 (2) and (c) $Fe_3O_4@SiO_2$-Dendrimer-Pd catalyst.

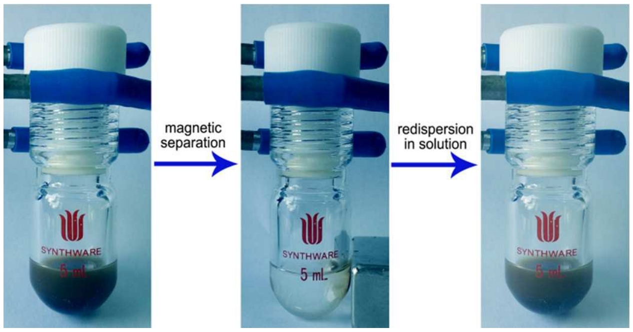

Fig. 4 The photograph of magnetic separation and redispersion of $Fe_3O_4@SiO_2$-Dendrimer-Pd catalyst.

Fig. 5 shows the TEM images of (a) $Fe_3O_4@SiO_2$, (b) $Fe_3O_4@SiO_2$-MA2-NH_2(2), (c) $Fe_3O_4@SiO_2$-Dendrimer-Pd and EDX image of $Fe_3O_4@SiO_2$-Dendrimer-Pd. As can be seen all the magnetic nanoparticles are quasi spherical with average diameters of about 13.9 nm, 15.6 nm and 16.1 nm, respectively. In addition, the EDX image clearly shows the presence of palladium, suggesting the $Fe_3O_4@SiO_2$-Dendrimer-Pd catalyst has been prepared successfully.

The X-ray diffraction (XRD) patterns of (a) $Fe_3O_4@SiO_2$, (b) $Fe_3O_4@SiO_2$-MA2-NH_2(2) and (c) $Fe_3O_4@SiO_2$-Dendrimer-Pd catalyst were shown in Fig. 6. It can be seen that all the samples show six same diffraction peaks with 2θ of 30.1°, 35.4°, 43.5°, 53.5°, 56.8° and 62.8°, corresponding to the crystal faces (220), (311), (400), (422) , (511) and (440) of Fe_3O_4 (JCPDS file No. 19-0629) . In Fig. 5c ,

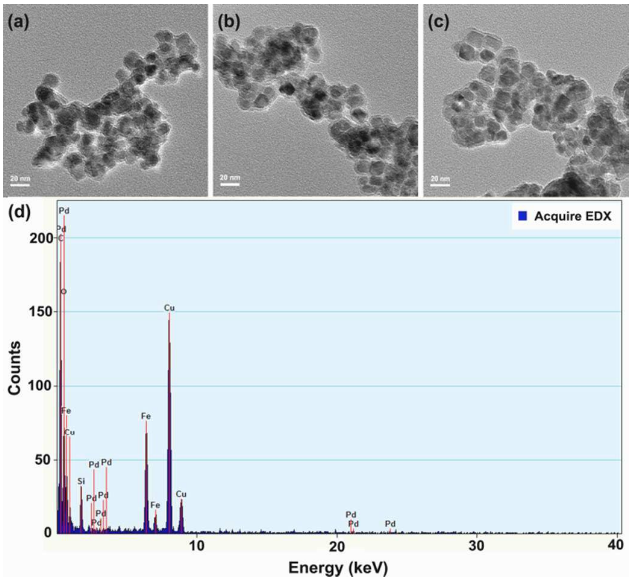

Fig. 5 TEM images of (a) $Fe_3O_4@SiO_2$, (b) $Fe_3O_4@SiO_2$-MA2-NH_2 (2) and (c) $Fe_3O_4@SiO_2$-Dendrimer-Pd and EDX image of (d) $Fe_3O_4@SiO_2$-Dendrimer-Pd .

View Article Online
DOI: 10.1039/C7NJ05014C

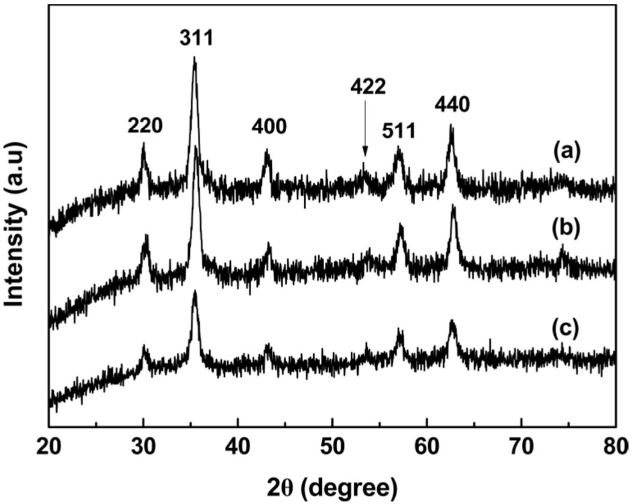

Fig. 6 XRD patterns of (a) $Fe_3O_4@SiO_2$, (b) $Fe_3O_4@SiO_2$-MA2-NH_2(2) and (c) $Fe_3O_4@SiO_2$-Dendrimer-Pd catalyst.

the diffraction peaks of Pd nanoparticles do not appear, probably because the palladium is not in the form of Pd nanoparticles or the content of Pd nanoparticles in the catalyst is low.[16]

To further investigate the oxidation state of immobilized palladium in the fresh and the used $Fe_3O_4@SiO_2$-Dendrimer-Pd catalyst, X-ray photoelectron spectroscopy (XPS) was conducted, and the results were shown in Fig. 7. In Fig. 6a, two characteristic peaks at the binding energies of 342.6 eV and 337.5 eV match well with the $3d_{3/2}$ and $3d_{5/2}$ peaks of Pd (II),[20a] indicating that the chemical state of palladium is divalent in the fresh $Fe_3O_4@SiO_2$-Dendrimer-Pd catalyst. In Fig. 6b, there are two new peaks appearing at the binding energies of 340.3 eV and 334.8 eV besides the peaks of Pd(II), which correspond to Pd(0)$3d_{3/2}$ and Pd(0)$3d_{5/2}$, respectively.[22] This result indicates that both Pd(II) and Pd(0) exist in the used $Fe_3O_4@SiO_2$-Dendrimer-Pd catalyst. The quantify of Pd(II) and Pd(0) were calculated to be about 45% and 55% respectively by XPS.

Initially, the Mizoroki-Heck reaction of iodobenzene with methylacrylate in the presence of $Fe_3O_4@SiO_2$-Dendrimer-Pd catalyst was chosen as the model reaction for optimization of different reaction conditions including the base, catalyst loading and solvent types (Table 2). The model reaction was first performed using different bases such as NaOAc, K_2CO_3, n-Bu_3N and Et_3N, amongst them Et_3N was more appropriate for the Mizoroki-Heck reaction and gave the highest yield of 96% (entries 1-4). Next, the effect of the catalyst loading was also explored in the model reaction (entries 4-6), and the result showed that 0.009 mol% Pd was the appropriate catalyst dosage for the Mizoroki-Heck reaction. Finally, solvent-free system was the most favorable system among solvent-free, H_2O and DMF owing to its green and low-cost (entries 4, 7, 8).

Futhermore, the reaction kinetics of the Mizoroki-Heck reaction of iodobenzene with methylacryate were investigated. As shown in Fig. 8, the isolated yield of *trans*-methyl cinnamate increased quickly with reaction time until it reached 96% at 40 min. However, when further prolong the reaction time to 60 min, the isolated yield did not increase any more, indicating that 40 min is enough for the solvent-free Mizoroki-Heck reaction.

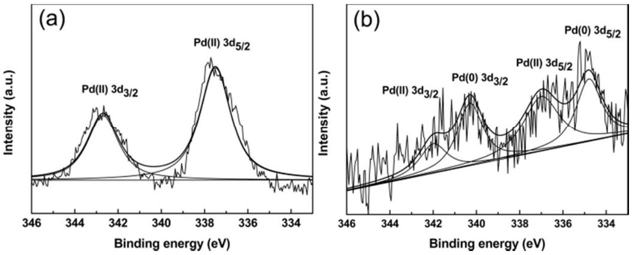

Fig. 7 XPS spectra of (a) fresh $Fe_3O_4@SiO_2$-Dendrimer-Pd catalyst and (b) $Fe_3O_4@SiO_2$-Dendrimer-Pd catalyst after one run in Mizoroki-Heck reaction.

Table 2 Optimization of the Mizoroki-Heck reaction of iodobenzene with methylacrylate catalyzed by $Fe_3O_4@SiO_2$-Dendrimer-Pd[a]

Entry	Base	Catalyst[b]	solvent	Yield[c] (%)
1	NaOAc	0.009	-	Trace
2	K_2CO_3	0.009	-	Trace
3	n-Bu_3N	0.009	-	89%
4	Et_3N	0.009	-	96%
5	Et_3N	0.018	-	97%
6	Et_3N	0.0045	-	87%
7	Et_3N	0.009	H_2O	61%
8	Et_3N	0.009	DMF	97%

[a] Reaction conditions: iodobenzenen (2.0 mmol), methylacrylate (3.0 mmol), base (3.0 mmol), solvent (6.0 mL), 120 °C, 40 min. [b] Catalyst (based on iodobenzenen). [c] Isolated yield.

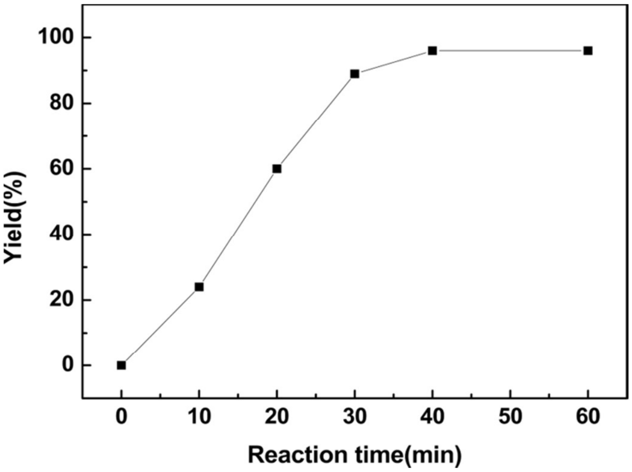

Fig. 8 Kinetic profiles of the $Fe_3O_4@SiO_2$-Dendrimer-Pd catalyst in the Mizoroki-Heck reaction. Reaction conditions: iodobenzene (2.0 mmol), methylacrylate (3.0 mmol), Et_3N (3.0 mmol), $Fe_3O_4@SiO_2$-Dendrimer-Pd (0.009 mol%), 120 °C.

With the optimized reaction conditions in hand (Et_3N, 0.009 mol% Pd, solvent-free, 40 min), the generality and versatility of $Fe_3O_4@SiO_2$-Dendrimer-Pd catalyst in solvent-free Mizoroki-Heck reactions of various aryl halides with olefins were investigated, and the results were shown in Table 3. Under the optimized conditions, various aryl iodides containing electron-withdrawing and electron-donating groups reacted efficiently with methylacrylate to afford excellent isolated yields and high TOF values (entries 2,3,5,6). The results showed that the iodobenzene with -CH_3 group gave lower yield than that with -Br, -Cl, -OCH_3 groups, which is mainly because groups with a lone electron pair (e.g. -Br , -Cl , -OH, -OCH_3)

View Article Online
DOI: 10.1039/C7NJ05014C

Table 3 Solvent-free Mizoroki-Heck reactions of aryl halides with olefins catalyzed by $Fe_3O_4@SiO_2$-Dendrimer-Pd [a]

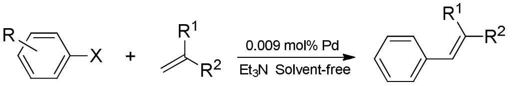

Entry	Aryl halides	Alkenes	Time	Yield [b]	TOF [c] (h^{-1})
1	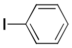		40 min	96%	16000
2	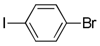		40 min	98%	16333
3	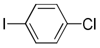		40 min	98%	16333
4	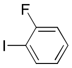		40 min	92%	15333
5	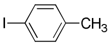		40 min 60min 80min	73% 85% 91%	12167 9444 7583
6	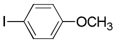		40 min	99%	16500
7	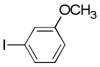	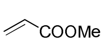	40 min	92%	15333
8	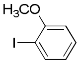	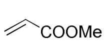	40 min	88%	14667
9		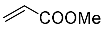	180 min	98%	3630
10	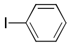		60 min	96%	10667
11	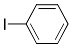		60 min	97%	10778
12	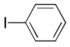	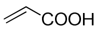	40 min	94%	15667
13	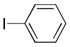		210 min	90%	2857
14	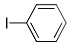		120 min	92%	5111
15	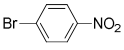		12 h	79[d]%	73

[a] Reaction conditions: aryl halides (2.0 mmol), olefins (3.0 mmol), Et_3N (3.0 mmol), $Fe_3O_4@SiO_2$-Dendrimer-Pd(0.009 mol%), 120 °C. [b] Isolated yields. [c] TOF: [molproduct][mol Pd]$^{-1}$ h^{-1}. [d] $Fe_3O_4@SiO_2$-Dendrimer-Pd(0.09 mol%).

in the iodobenzenes affect the electron cloud density of benzene ring and the coordination of Pd with the benzene ring, accelerating reaction rate.[23] Moreover, steric hindrance has played an important role in Mizoroki-Heck reaction. For methoxy-substituted aryl iodides, the para-methoxy iodide gave the highest yield of 99%, followed by *meta*-methoxy iodide and *ortho*-methoxy iodide. Notably, the large steric hindrance 1-iodonaphthalene (entry 9) was readily converted to the corresponding product in 98% yield despite that 180 min was required. The catalyst $Fe_3O_4@SiO_2$-Dendrimer-Pd also exhibited excellent catalytic activity toward different olefins (enties 1, 10-14). The coupling of methylacrylate and acrylic acid with iodobenzene gave the desired products in 96% and 94% yields, respectively. For steric hindrance olefins (ethyl acrylate, n-butyl acrylate, methyl methacrylate, styrene), the coupling reactions were carried out in a longer times to afford corresponding products in 90%-97% yields. Encouraged by the high efficiency of $Fe_3O_4@SiO_2$-Dendrimer-Pd in the reactions between aryl iodides with olefins, the catalyst was then applied in the solvent-free Mizoroki-Heck reaction of 4-bromonitrobenzene with methylacrylate using a 0.09 mol% Pd loading. A satisfactory yield of 79% was obtained by prolonging reaction time to 12 h.

In view of the excellent catalytic activity of $Fe_3O_4@SiO_2$-Dendrimer-Pd in solvent-free Mizoroki-Heck reactions, we investigated the potential of this catalyst in Suzuki-Miyaura coupling reactions in EtOH/H_2O solution. As shown in Table 4, aryl bromides containing electron-withdrawing groups and electron-donating groups reacted with arylboronic acids very well and generated the desired products with excellent yields (87%-98%) (entries 2-5). For the methyl-substituted aryl bromides (entries 5-7), the position and amount of the methyl group have a large influence on the reactions. The best result was obtained when the methyl group was in *para* position, followed by the *meta* and *ortho* positions. The worst result is the reaction between 3,5-dimethylbromobenzene and phenylboronic acid, and gave corresponding biaryl product in 87% yield. It is worth mentioning that the Suzuki-Miyaura reactions of inactivated-aryl chlorides with arylboronic acids could also proceed smoothly using only 0.009 mol% Pd loading within 8 h. 4-chlorobenzoic acid and 4-chloronitrobenzene were readily converted to corresponding biary products in 84% and 90% yields, respectively.

A comparison was also made with some supported Pd catalysts

Table 4 Suzuki-Miyaura reactions between aryl halides and phenylboronic acid in the presence of $Fe_3O_4@SiO_2$-Dendrimer-Pd catalyst[a]

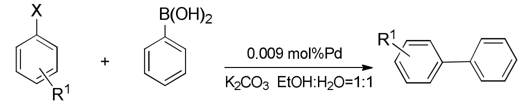

Entry	Aryl halides	Arylboronic acid	Time	Yield[b]	TOF [c]/h^{-1}
1	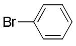	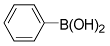	1 h	97%	10778
2	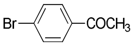	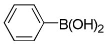	1 h	98%	10889
3	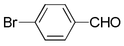	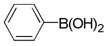	1 h	97%	10778
4	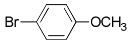	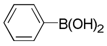	1 h	93%	10333
5	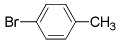	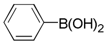	1 h	96%	10667
6	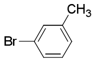	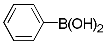	1 h	94%	10444
7	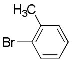	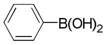	1 h	90%	10000
8	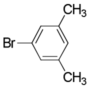	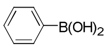	1 h	87%	9667
9	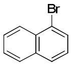	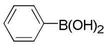	1h	96%	10667
10	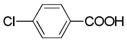	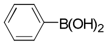	8 h	84%	1167
11	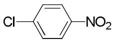	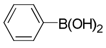	8 h	90[d]%	1250

[a] Reaction conditions: phenylboronic acid (2.4 mmol), K_2CO_3 (5.0 mmol), solvent (6.0 mL, EtOH：H_2O=1:1), $Fe_3O_4@SiO_2$-Dendrimer-Pd(0.009 mol%), 75 °C. [b] Isolated yields. [c] TOF: [molproduct][molPd]$^{-1}$$h^{-1}$. [d] 2mmol TBAB.

View Article Online
DOI: 10.1039/C7NJ05014C

Table 5 Performance of various supported Pd catalysts in solvent-free Mizoroki-Heck reaction between iodobenzene and methylacrylate

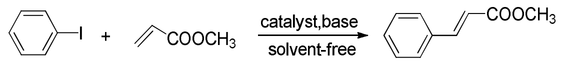

Entry	Pd catalyst /mol%	Base/temperature/time	Yield[a]	TOF[b] /h^{-1}	Ref
1	Fe_3O_4@SiO_2-Dendrimer-Pd (0.009)	Et_3N/120 °C /40 min	96%	16000	This work
2	polystyrene-anchored Pd(II) phenyldithiocarbazate complex (1)	Et3N/70 oC /5 h	95%	19	24
3	PDVB-IL-Pd (0.02)	Et3N/120 oC /4 h	97c %	1213	25
4	SBA-TMG-Pd (0.01)	Et3N/140 oC /65 min	91%	8400	26
5	D-glucosamine-derived triazole@Pd (0.1)	Et3N/80 oC /6 h	93%	155	27
6	Pd-DABCO-γ-Fe_2O_3 (1)	Et3N/100oC /0.5 h	90%	180	28
7	Pd/Fe_3O_4@PIL-NH_2 (0.011)	Et3N/120 oC /25 min	94%	20509	29

[a] Isolated yields. [b] TOF: [molproduct][mol Pd]$^{-1}$ h^{-1}.

reported to further evaluate the catalytic activity of Fe_3O_4@SiO_2-Dendrimer-Pd catalyst in solvent-free Mizoroki-Heck reaction of iodobenzene and methylacrylate. As shown in Table 5, the coupling reaction proceeded efficiently using only 0.009 mol% Fe_3O_4@SiO_2-Dendrimer-Pd catalyst, and high TOF values of up to 16000 h^{-1} have been achieved. This result is obviously superior most supported Pd catalysts except magnetic poly (ionic liquid) supported Pd catalyst Pd/Fe_3O_4@PIL-NH_2 (entries 1-7), but Fe_3O_4@SiO_2-Dendrimer-Pd catalyst can be prepared with the lower cost, the milder conditions and easier operation. From the aspects of practical consideration, Fe_3O_4@SiO_2-Dendrimer-Pd is efficient and economic supported Pd catalyst.

Recyclability and reusability of supported Pd catalysts is one of the most important issues from practical, economical and environmental points of view. In order to investigate the reusability of Fe_3O_4@SiO_2-Dendrimer-Pd, the solvent-free Mizoroki-Heck reaction of iodobenzene with n-butyl acrylate was chosen as the model reaction. After each run, the Fe_3O_4@SiO_2-Dendrimer-Pd catalyst was magnetically separated, washed with ethyl acetate/ethanol (1:1, v/v) and dried for next use. As shown in Table 6 , this catalyst could be used consecutively for five times with still 88% yield achieved. The content of palladium leaching was determined to be 0.06 ppm in the solution of fifth run based on AAS, indicating this catalyst was stable during the solvent-free Mizoroki-Heck reactions.

Table 6 Recycling and reuse of Fe_3O_4@SiO_2-Dendrimer-Pd in the solvent-free Mizoroki-Heck reaction[a]

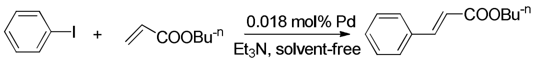

Run	1	2	3	4	5
Yield[b]	97%	97%	95%	93%	88%

[a] Reaction conditions: Reaction conditions: iodobenzene (1.0 mmol), n-butyl acrylate (1.5 mmol), Et_3N (1.5 mmol), Fe_3O_4@SiO_2-Dendrimer-Pd (0.018 mol% Pd), 120 °C, 60 min. [b] Isolated yields.

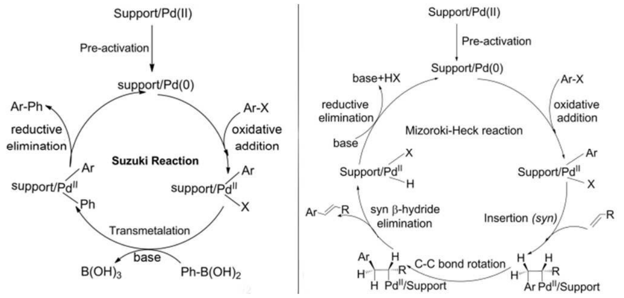

Scheme 2 Proposed mechanism for the Suzuki-Miyaura and Mizoroki-Heck cross-coupling reactions in the presence of Fe_3O_4@SiO_2-Dendrimer-Pd catalyst.

In order to investigate catalytic mechanism in our reaction system, hot filtration test for the Mizoroki-Heck reaction of iodobenzene with methyl acrylate and Suzuki-Miyaura reaction of bromobenzene with phenylboronic acid under the optimized reaction conditions were performed. For the Mizoroki-Heck reaction, the reaction was stopped after 10 min and gave the corresponding product in 25% yield. In addition, when the catalyst was filtered off after 10 min and the filtrate was allowed to react for another 30 min, 29% yield was obtained. For the Suzuki-Miyaura reaction, the reaction was stopped after 25 min and gave the corresponding biphenyl product in 60% yield. In addition, when the catalyst was filtered off after 25 min and the filtrate was allowed to react for another 35 min, 63% yield was obtained. Above results revealed that the palladium leaching was negligible in both Mizoroki-Heck and Suzuki-Miyaura reactions, demonstrating the palladium deposited on Fe_3O_4@SiO_2-MA2-NH_2(2) dendritic polymers act as a heterogeneous catalyst in both the reactions. Plausible mechanisms for the Mizoroki-Heck and Suzuki-Miyaura reactions, based on previous reports, are proposed in Scheme 2.[30]

4 Conclusion

In conclusion, we have developed a novel magnetic dendritic polymer nanocomposites-supported palladium catalyst Fe_3O_4@SiO_2-Dendrimer-Pd, which could efficiently catalyze Mizoroki-Heck reaction in solvent-free condition and Suzuki-Miyaura reaction in EtOH/H_2O solvent, being in line with the development requirements of green chemistry. In addition, this catalyst can be easily removed from reaction mixture with an external magnet and consecutively recycled for five times with excellent yields achieved. These results may provide crucial information and insight for the future design of environmentally friendly catalytic system with excellent catalytic activity.

Conflicts of interest

There are no conflicts to declare.

Acknowledgements

View Article Online
DOI: 10.1039/C7NJ05014C

We gratefully acknowledge financial support from the National Science Foundation for Fostering Talents in Basic Research of the National Natural Science Foundation of China (J1103307).

Notes and references

1 (a) A. Molnar, *Chem. Rev.*, 2011, 111, 2251-2320; (b) K. Balinge, A. Khiratkar and P. Bhagat, *J. Organomet. Chem.*, 2018, 854, 131-139; (c) S. Layek, Anuradha, B. Agrahari, D. Pathak, *J. Organomet. Chem.*, 2017, 846, 105-112; (d) B. Agrahari, S. Layek, Anuradha, R. Ganguly, D. Pathak, *Inorg. Chim. Acta,* 2018, 471, 345-354.

2 (a) B. Karimi, F. Mansouri and H. M. Mirzaei, *ChemCatChem*, 2015, 7, 1736-1789; (b) Anuradha, S. Kumari, S. Layeka and D. Pathak, *New J. Chem*., 2017, 41, 5595-5604.

3 N. T. Phan, M. Sluys and C. W. Jones, *Adv. Synth. Catal.*, 2006, 348, 609-679.

4 D. Wang, C. Deraedt, J. Ruiz and D. Astruc, *Acc. Chem. Res.*, 2015, 48, 1871-1880.

5 J. H. Noh and R. Meijboom, *J. Colloid Interface Sci.*, 2014, 415, 57-69.

6 M. Esmaeilpour, A. Sardarian and J. Javidi, *Catal. Sci. Technol.*, 2016, 6, 4005-4019.

7 C. Deraedt, D. Wang, L. Salmon, L. Etienne, C. Labrugère, J. Ruiz and D. Astruc, *ChemCatChem*, 2015, 7, 303-308.

8 C. Deraedt, L. Salmon, L. Etienne, J. Ruiz and D. Astruc, *Chem. Commun.*, 2013, 49, 8169-8171.

9 Z. Gao, J. Qiu, Y. Pang and J. Sun, *Chem. Eng.*, 2012, 6, 29-32.

10 (a) D. Astruc, F. Lu and J. R. Aranzaes, *Angew. Chem., Int. Ed.*, 2005, 44, 7852-7872; (b) B. Li, Y. Yu, P. Zhao and S. Zhang, *Chem. Asian J.,* 2016, 11, 3550-3556; (c) D. Wang, C. Deraedt, L. Salmon, C. Labrugére, L. Etienne, J. Ruiz and D. Astruc, *Chem. Eur. J.*, 2015, 21, 1508-1519; (d) M. pirhayati, H. Veisi and A. Kakanejadifard, *RSC Adv.*, 2016, 6, 27252-27259.

11 C. Deraedt, L. Salmon, D. Astruc, *Adv. Synth. Catal.*, 2014, 356, 2525-2538.

12 L. M. Rossi, N. J. Costa, F. P. Silva and R. Wojcieszak, *Green Chem*., 2014, 16, 2906.

13 M. Quirin, Kainz and R. Oliver, *Acc. Chem. Res.*, 2014, 47, 667-677.

14 D. Wang, C. Deraedt, L. Salmon, C. Labrugere, L. Etienne, J. Ruiz and D. Astruc, *Chemistry*, 2015, 21, 1508-1519.

15 D. Rosario-Amorin, M. Gaboyard, R. Clerac, S. Nlate, K. Heuze, *Dalton Trans.*, 2011, 40, 44-46.

16 (a) P. Yang, R. Ma and F. Bian, *ChemCatChem.*, 2016, 8, 3746-3754; (b) Y. L. Li, Z. Q. Zhang, J. F. Shen and M. X. Ye, *Dalton Trans.*, 2015, 44, 16592-16601.

17 J. Wang, S. Zheng, Y. Shao, J. Liu, Z. Xu and D. Zhu, *J. Colloid Interface Sci.*, 2010, 349, 293-299.

18 J. M. Zhang, S. R. Zhai, B. Zhai, Q. D. An and G. Tian, *J. Sol-Gel Sci. Technol.*, 2012, 64, 347-357.

19 Y. Wang, P. Su, S. Wang, J. Wu, J. Huang and Y. Yang, *J. Mater. Chem. B*, 2013, 1, 5028.

20 (a) A. Gniewek, A. Trzeciak, J. Ziolkowski, L. Kepinski, J. Wrzyszcz and W. Tylus, *J. Catal.*, 2005, 229, 332-343; (b)M.R.Nabid, Y. Bide and S. J. Rezaei, *Appl. Catal. A*, 2011, 406, 124-132.

21 (a) G. He, C. Zhu, S. Ye, W. Cai, Y. Yin, H. Zhen and Y. Yi, *Int. J. Biol. Macromol.*, 2016, 91, 828-837; (b) I. Kohsari, Z. Shariatinia and S. Pourmortazavi, *Carbohydr. Polym*., 2016, 140, 287-298; (c) Anuradha, S. Kumari, S. Layeka and D. Pathak, *New J.Chem.*, 2017, 41, 5595-5604.

22 R. Li, P. Zhang, Y. Huang, P. Zhang, H. Zhong and Q. Chen, *J. Mater. Chem.*, 2012, 22, 22750.

23 G. Liu, M. Hou, J. Song, T. Jiang, H. Fan, Z. Zhang and B. Han, *Green Chem.*, 2010, 12, 65-69.

24 M. Bakherad, A. Keivanloo and S. Samangooei, *Tetrahedron Lett.*, 2012, 53, 5773-5776.

25 G. Liu, M. Hou, J. Song, T. Jiang, H. Fan, Z. Zhang and B. Han, *Green Chem.*, 2010, 12, 65-69.

26 X. Ma, Y. Zhou, J. Zhang, A. Zhu, T. Jiang and B. Han, *Green Chem*., 2008, 10, 59-66.

27 C. Shen, H. Shen, M. Yang, C. Xia and P. Zhang, *Green Chem.*, 2015, 17, 225-230.

28 S. Sobhani and Z. Pakdin-Parizi, *Appl. Catal. A*, 2014, 479, 112-120.

29 W. Liu, D. Wang, Y. Duan, Y. Zhang and F. Bian, *Tetrahedron Lett.*, 2015, 56, 1784-1789.

30. N. Phan, M. Sluys and C. Jones, Adv. Synth. Catal., 2006, 348, 609-679.